Seelig, J., & Seelig, A. (1980) *Q. Rev. Biophys. 13*, 19–61.
Seelig, J., Tamm, L., Hymel, L., & Fleischer, S. (1981) *Biochemistry 20*, 3922–3932.
Shinitzky, M., & Barenholz, Y. (1978) *Biochim. Biophys. Acta 515*, 367–394.
Sklar, L. A., Miljanich, G. P., Bursten, S. L., & Dratz, E. A. (1979) *J. Biol. Chem. 254*, 9583–9591.
Slater, T. F. (1984) *Methods Enzymol. 105*, 283–293.
Smith, H. G., Stubbs, G. W., & Litman, B. J. (1975) *Exp. Eye Res. 20*, 211–217.
Smith, H. G., Fager, R. S., & Litman, B. J. (1977) *Biochemistry 16*, 1399–1405.
Straume, M., & Litman, B. J. (1987a) *Biochemistry 26*, 5113–5120.
Straume, M., & Litman, B. J. (1987b) *Biochemistry 26*, 5121–5126.
Stubbs, C. D. (1983) *Essays Biochem. 19*, 1–39.
Stubbs, C. D., Kouyama, T., Kinosita, K., Jr., & Ikegami, A. (1981) *Biochemistry 20*, 4257–4262.
Stubbs, C. D., Kinosita, K., Jr., Munkonge, F., Quinn, P. J., & Ikegami, A. (1984) *Biochim. Biophys. Acta 775*, 374–380.
Stubbs, G. W., & Litman, B. J. (1978) *Biochemistry 17*, 220–225.
Stubbs, G. W., Litman, B. J., & Barenholz, Y. (1976) *Biochemistry 15*, 2766–2772.
Sunamoto, J., Baba, Y., Iwamoto, K., & Kondo, H. (1985) *Biochim. Biophys. Acta 833*, 144–150.
Szabo, A. (1984) *J. Chem. Phys. 81*, 150–167.
Thompson, T. E., & Huang, C. (1986) in *Physiology of Membrane Disorder*, 2nd ed. (Andrioli, T. E., Hoffman, J. F., Fanestil, D. D., & Schultz, S. G., Eds.) pp 25–44, Plenum, New York.
Utsumi, H., Tunggal, B. D., & Stoffel, W. (1980) *Biochemistry 19*, 2385–2390.
van Blitterswijk, W. J., van Hoevan, R. P., & van der Meer, B. W. (1981) *Biochim. Biophys. Acta 644*, 323–332.
van der Meer, W., Pottel, H., Herreman, W., Ameloot, M., Hendrickx, H., & Schroder, H. (1984) *Biophys. J. 46*, 515–523.
van de Ven, M., van Ginkel, G., & Levine, Y. K. (1984) *Biochem. Biophys. Res. Commun. 123*, 352–357.
Vogel, H., & Jahnig, F. (1985) *Proc. Natl. Acad. Sci. U.S.A. 82*, 2029–2033.
Vos, M. H., Kooyman, R. P. H., & Levine, Y. K. (1983) *Biochem. Biophys. Res. Commun. 116*, 462–468.
Wang, S., Glaser, M., & Gratton, E. (1986) *Biophys. J. 49*, 307a.
Wong, P. T. T. (1984) *Annu. Rev. Biophys. Bioeng. 13*, 1–24.
Yeagle, P. L. (1984) *Prog. Clin. Biol. Res. 159*, 153–175.
Zannoni, C., Arcioni, A., & Cavatorta, P. (1983) *Chem. Phys. Lipids 32*, 179–250.
Zumbulyadis, N., & O'Brien, D. F. (1979) *Biochemistry 18*, 5427–5432.

Rotational Dynamics of Actin†

William H. Sawyer,* Amanda G. Woodhouse, Joseph J. Czarnecki,‡ and Edward Blatt§
Russell Grimwade School of Biochemistry, University of Melbourne, Parkville, Victoria 3052, Australia
Received November 13, 1987; Revised Manuscript Received June 9, 1988

ABSTRACT: The rotational diffusion of actin was studied with the technique of time-resolved phosphorescence anisotropy using actin labeled at Cys-374 with erythrosin iodoacetamide. Immediately after the polymerization of actin was initiated, the correlation time increased sharply, passing through a maximum at 5 min and then declined to low values. F-Actin at equilibrium showed no anisotropy decay. The results were interpreted as indicating the initial formation of short mobile filaments which became increasingly immobile as elongation proceeded, leaving a decay which was dominated by shorter filaments. Some of these short filaments could have arisen by fragmentation of longer filaments. Eventually, the shorter filaments themselves became immobilized by entanglement within the gel matrix. The infinite-time anisotropy increased during polymerization, reflecting a smaller range of angular motion of the probe brought about by restricted torsional motion on the submicrosecond time scale. The results were compared with the length distribution of actin filaments revealed by electron microscopy [Kawamura, M., & Maruyama, K. (1970) *J. Biochem.* (*Tokyo*) *67*, 437–457]. Polymerization in the presence of 1 μM cytochalasin B abolished the maximum in the correlation time profile and tended to prevent the immobilization of filaments by favoring shorter capped filaments which retained considerable rotational freedom. Addition of spectrin dimer to F-actin caused an increase in the time-invariant anisotropy. Subsequent additions of spectrin-binding proteins (erythrocyte bands 2.1 and 4.1) caused further increases in the anisotropy in a concentration-dependent manner, suggesting additional restriction of submicrosecond torsional motions. The results suggest that actin filaments within nonmuscle cells are rotationally immobile particularly if they are cross-linked by actin-binding proteins.

Microtubules, intermediate filaments, and microfilaments play an important role in determining cell shape and motility and the disposition and movement of subcellular organelles. Together with their associated proteins, they make up a cytoskeletal scaffolding on which is arrayed a number of cytoplasmic enzymes. Although the term "cytoskeleton" implies a relatively rigid arrangement of structural units of limited flexibility, it is more likely that cytoskeletal elements possess degrees of internal and global motion that permit deformation of cell shape without rupture of the cell membrane and

† This work was supported by the Australian Research Grants Scheme.
‡ Present address: ICI Diagnostics, 5 Guest St., Hawthorn, Victoria 3122, Australia.
§ Present address: CSIRO Division of Applied Organic Chemistry, GPO Box 4331, Melbourne, Victoria 3001, Australia.

0006-2960/88/0427-7733$01.50/0

fragmentation of the cytoskeleton itself. Of prime importance is the internal flexibility of the actin microfilament with respect to both torsional and bending motions. In addition, the rotational and translational diffusion coefficients are also important parameters of microfilament motion since they may reflect the structural dynamics of the cytoskeletal system as a whole.

The translational diffusion of the actin microfilament has been studied extensively by the technique of fluorescence recovery after photobleaching (Lanni et al., 1981; Tait & Frieden, 1982a,b; Lanni & Ware, 1984; Mozo-Villarias & Ware, 1985). The polymerization of actin brings about an increase in the recovery time as well as a decrease in the proportion of fluorescence recovered. Before the completion of polymerization, the filaments become completely immobile as far as translational motion is concerned. The degree of immobilization depends on the solvent conditions and appears to be more pronounced when 2.0 mM $MgCl_2$ is used to initiate polymerization compared to 50 mM KCl (Tait & Frieden, 1982a,b; Lanni & Ware, 1984). Application of a shear stress causes breakage of filaments with a consequent decrease in the fraction of immobilized actin. The actin returns to its fully immobile state after a period of annealing (Tait & Frieden, 1982a). The persistence length of actin is relatively long (6–25 μm; Osawa, 1980). Since the majority of filaments are shorter than this length (Kawamura & Maruyama, 1970), their diffusion should be similar to that predicted for a rigid rod. The translational diffusion of F-actin is much slower than that expected on this basis, and it is concluded that the observed immobilization is due to intermeshing of fibers as well as to physical contact between them. Indeed, side-by-side and crossover points of contact have been observed in electron micrographs of actin filament networks (Neiderman et al., 1983).

The rotational diffusion of F-actin arises from internal torsional motions as well as from the uniaxial motion of the filament as a whole. The torsional motion is relatively fast and has been detected by fluorescence anisotropy techniques (Mihashi & Wahl, 1975; Wahl et al., 1975; Kawasaki et al., 1976). Tawada et al. (1978) and Ikkai et al. (1979) resolved four correlation times in the anisotropy decay of actin labeled with *N*-(iodoacetyl)-*N'*-(5-sulfo-1-naphthyl)ethylenediamine at Cys-374. The shortest correlation time (6 ns) was attributed to fast local motion within the actin monomer unit. The second decay (45 ns) was consistent with the global motion of monomer units in equilibrium with the polymer. The third (100 ns) and fourth (900 ns) decays were attributed to torsional motion within the filament since they were much shorter than the correlation time expected for the uniaxial motion of the filament as a whole (e.g., 43 μs for a filament 1 μm in length).

In this paper, we direct attention to the relatively slow rotational motion of the growing actin filament which occurs on the millisecond to microsecond time scale. The anisotropy of phosphorescence decay is ideal for detecting rotational diffusion over this time window (Austin et al., 1979; Jovin et al., 1981). Of particular importance is the question of whether actin filaments are free to rotate or whether their rotation is hindered by the intermeshing and physical contact with neighboring filaments. It will be shown that actin gels are rotationally immobile on this time scale but that during the nucleation and elongation steps of polymerization the kinetics of the anisotropy decay reflect the length distribution of filaments. The angular motion of the phosphorescence probe becomes more restricted when actin-binding proteins such as erythrocyte spectrin are added to the system, and when the spectrin itself is bound to components 4.1 and 2.1 isolated from the erythrocyte membrane.

Materials and Methods

Materials. Glucose oxidase and ATP were obtained from Boehringer Mannheim, and erythrosin 5-iodoacetamide was from Molecular Probes (Oregon). Glycerol (Merck) was of a grade used for fluorescence microscopy. The viscosities of glycerol solutions were obtained from Timmermans (1960). Bovine serum albumin and rabbit muscle aldolase were purchased from Sigma Chemical Co. Spectrin dimers were prepared from human erythrocytes by the method of Cohen and Foley (1980). A preparation containing bands 2.1 and 4.1 (1:1 w/w) was prepared by high-salt extraction of spectrin–actin-depleted erythrocyte vesicles (Sawyer et al., 1983).

Actin Preparation. Actin was prepared from rabbit muscle by the method of Spudich and Watt (1971). It was purified by repeated G to F cycles, and the resulting material was freeze-dried in the presence of sucrose. Actin was dialyzed against buffer G (2 mM Tris-HCl, 0.2 mM $CaCl_2$, 0.2 mM ATP, and 0.002% NaN_3, pH 8.0) and was recycled through the F form before use. G-Actin was stored on ice in buffer G adjusted to pH 7.6 and used within 4 days of preparation.

Actin Labeling. G-Actin was clarified by centrifugation at 300000*g* for 80 min and dialyzed overnight against buffer F (buffer G at pH 7.6 plus 50 mM KCl and 2 mM $MgCl_2$). Erythrosin iodoacetamide was dissolved in dimethylformamide and a small volume (37 μL) added to 2.0 mL of buffer F. This was incubated with 1.0 mL of F-actin solution (probe:protein molar ratio of 2:1) for 2 h at room temperature in the dark. Unreacted dye was removed by sedimentation of F-actin (150000*g* for 1.5 h) followed by exhaustive dialysis against buffer G adjusted to pH 7.6. The labeled actin was cycled twice through the F and G forms and finally stored in the G form on ice in the dark. The labeling of actin with iodoacetamide derivatives of fluorophores is known to specifically label Cys-374 (Lanni & Ware, 1984). The molar ratio of dye to protein was determined spectrophotometrically and was usually in the range 0.70–0.95. The molar extinction coefficient of erythrosin was taken as 83 000 M^{-1} cm^{-1} at 539 nm (Moore et al., 1979). Spectral analysis of the dye conjugated to a molar excess of L-lysine showed that the absorbance of the dye at 290 nm was 29% of its absorbance at 539 nm; this correction was used to determine the protein concentration from the absorbance at 290 nm. Labeling to dye:protein ratios greater than 1 was found to impair the polymerizability of the actin. Aldolase and bovine serum albumin were labeled under similar conditions. All phosphorescence experiments were conducted at pH 7.6 in buffer G or buffer F. The polymerization of actin was initiated by the addition of $MgCl_2$ and KCl to concentrations of 2 and 50 mM, respectively. The concentration of labeled actin was within the range 45–55 μg/mL, with unlabeled actin being added to bring solutions to higher total actin concentrations.

Instrumentation and Data Analysis. Time-resolved phosphorescence measurements were carried out with instrumentation similar to that described by Austin et al. (1979). A dye laser (Molectron DL 10/14, coumarin dye) was driven by a pulsed nitrogen laser (Molectron UV 14, 1 mJ/pulse, 20 Hz) to deliver light of 515 nm and 8–10-ns pulse width. The laser beam, vertically polarized with an intracavity prism, illuminated the sample contained in a 7 × 7 mm cross-section cuvette. Oxygen was removed by including glucose oxidase (30 μg/mL) and glucose (130 mM) in the sample, and the surface of the sample was flushed with argon to maintain the oxy-

gen-free environment. The luminescence was collected at 90° to the direction of the laser beam and the phosphorescence isolated by a combination of RG695 and KV550 Schott cutoff filters. The phosphorescence of erythrosin occurs within the wavelength range 650–750 nm (Garland & Moore, 1979; Moore et al., 1979). A gated photomultiplier (EMI 9817 QBG) was used to collect the luminescence 1 μs after the laser pulse, thereby avoiding the intense spike of prompt fluorescence. Decays of the parallel [$I_{VV}(t)$] and perpendicular [$I_{VH}(t)$] components of the polarized transient phosphorescence were collected serially by 90° rotation of the emission polaroid after the collection of every 64th decay. A 1024-channel Nicolet 1170 signal averager was used to digitize the signal and accumulate 512 decays of each component. After subtraction of background signals, the decays were transferred to a PDP 11/23 computer and the total intensity [$I(t)$] and anisotropy [$r(t)$] curves generated according to the expressions:

$$I(t) = I_{VV}(t) + 2I_{VH}(t) \quad (1)$$

$$r(t) = I_{VV}(t) - I_{VH}(t)/[I_{VV}(t) + 2I_{VH}(t)] \quad (2)$$

Data collected in the first few microseconds after the laser flash were distorted probably due to jitter in the gate circuitry. Phosphorescence data collected prior to 4 μs were discarded in all cases. The integrity of the optics and electronics was tested by determining the ratio of the emission intensities obtained for excitation with horizontally polarized light, $G(t) = I_{HH}(t)/I_{HV}(t)$. Theoretically, this ratio should be unity. The experimentally determined value was 0.98 ± 0.01 and was independent of time provided that the excitation light was completely polarized in the horizontal direction. The generated curves were fitted to functions:

$$I(t) = \sum_i \alpha_i \exp(-t/\tau_i) + B \quad (3)$$

$$r(t) = \sum_j \beta_j \exp(-t/\phi_j) + r_\infty \quad (4)$$

α_i represents the initial intensity of the decay component i having a lifetime τ_i, and β_j is the partial anisotropy of component j associated with rotational correlation time ϕ_j; r_∞ is the infinite-time anisotropy. These decays were fitted by using a nonlinear least-squares iterative procedure based on the Marquardt algorithm (Bevington, 1969) or a Chebyshev transformation procedure (Malachowski & Ashcroft, 1987; De Boech et al., 1985). The latter was part of a data acquisition operating system (DAOS) supplied by Labsoft Associates (Melbourne). Goodness-of-fit was determined from values of the reduced χ^2 or from plots of the unweighted residuals (Restall et al., 1984). Up to four exponentials were required to fit total intensity decays and up to two to fit anisotropy decays. Triplicate data sets were collected for each sample, except for those experiments designed to follow the assembly of filaments with time when only one set was collected for each time point. Errors associated with the decay parameters are the standard deviations of triplicate measurements.

The rotational correlation time for a sphere of equivalent volume to a given protein was determined according to the relation:

$$\phi = \frac{\eta M}{RT}(\bar{v}_2 + \delta\bar{v}_0) \quad (5)$$

where η is the viscosity of the solvent, M is the molecular weight, $\bar{v}_2$ is the partial specific volume of the protein, $\bar{v}_0$ is the partial specific volume of water, and δ is the protein hydration, assumed to be 0.37 g/g (Kuntz, 1971).

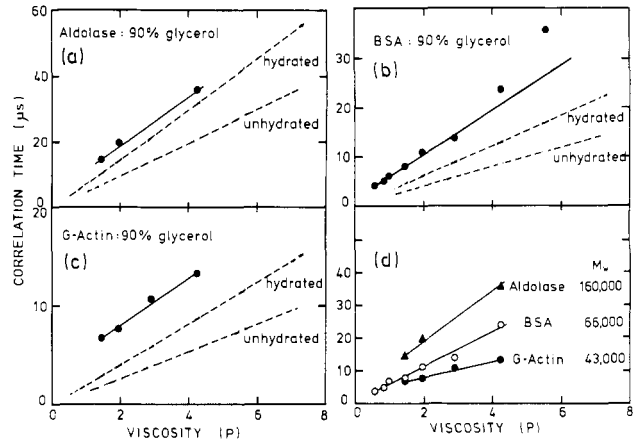

FIGURE 1: Dependence of the rotational correlation time on solvent viscosity for (a) aldolase, (b) bovine serum albumin, and (c) G-actin. The viscosity of glycerol was varied by changing the temperature. The theoretical correlation times for hydrated and unhydrated spheres of the same molecular weight as the proteins were calculated according to eq 5. The experimental data for the three proteins are compared in (d). The labeling ratios (mole:mole) were 0.83 for G-actin, 0.77 for aldolase, and 0.70 for bovine serum albumin. Protein concentrations were adjusted so that all solutions were 1 μM in erythrosin.

Results and Discussion

Globular Proteins in Glycerol. The rotational diffusion of several proteins in glycerol was measured to test the reproducibility of measurements and to examine the relationship between rotational diffusion and molecular size. The results are summarized in Figure 1 which shows the relationship between the rotational correlation time and the solvent viscosity for G-actin, aldolase, and bovine serum albumin. In all cases, the anisotropy decay was fitted by a single exponential function. Successive measurements of a single sample showed that the correlation time could be determined with an accuracy of 5%. The correlation time was greater than that expected for a hydrated sphere of the same molecular weight as the protein, the factors (±SD) being 1.65 ± 0.68 for aldolase, 1.98 ± 0.27 for BSA, and 1.97 ± 0.36 for G-actin. Similar ratios have been found in fluorescence anisotropy measurements of globular proteins in low-viscosity solvents (Yguerabide, 1972) and for absorption dichroism measurements of eosin-labeled proteins in high-viscosity solvents (Cherry & Schneider, 1976) and have been attributed to molecular asymmetry.

Actin. The phosphorescence of monomeric actin in solution is completely depolarized due to its rapid tumbling (Figure 2, trace ii). The anisotropy of F-actin is independent of time within the range 4–1000 μs and attains values of 0.035–0.08 depending on the age of the actin preparation and its concentration (Figure 2, trace i). Similar results were found for actin labeled with eosin iodoacetamide. Control experiments using unlabeled F-actin showed that scattering of the laser beam by filaments did not lead to polarization artifacts. Addition of spectrin dimer causes a doubling of the anisotropy (Figure 3), and addition of a preparation containing bands 2.1 and 4.1 causes further increases in anisotropy in a concentration-dependent manner (Figure 3). On each addition, the anisotropy remained independent of time within the phosphorescence time window. Bands 2.1 and 4.1 bind to opposite ends of the 100-nm-long spectrin dimer, and thus the bulk of the ternary complex with spectrin would be expected to limit the submicrosecond torsional motion of actin when bound to the filament. The apparent zero-time anisotropy (r_0) therefore increases toward the limit characteristic of the completely immobilized chromophore. Zidovetski et al. (1986) determined a limit of $r = 0.21$ for erythrosin immobilized in a glass of

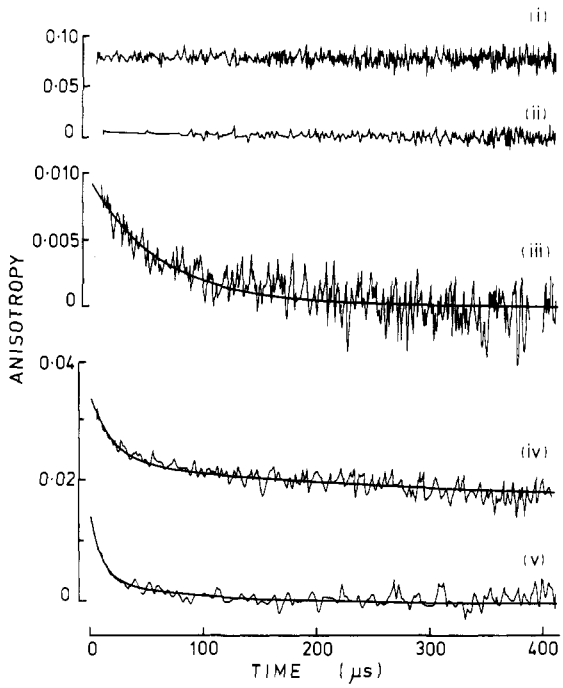

FIGURE 2: Time-resolved anisotropies of (i) F-actin and (ii) G-actin at a protein concentration of 1.0 mg/mL (25 °C). Trace iii is the anisotropy of actin (1.0 mg/mL) measured 5 min after the initiation of polymerization at 13.0 °C. The smooth line is the computer fit to a single exponential function for the parameters ϕ = 60 μs, r_0 = 0.009, r_∞ = 0.001. Traces iv and v are the anisotropy decays of actin in the presence of 1 μM cytochalasin B measured 5 and 40 min after the initiation of polymerization. The smooth lines are the computer fits to a two-exponential function (eq 4) with the following parameters: trace iv, ϕ_1 = 10.8 μs, ϕ_2 = 104.0 μs, β_1 = 0.011, β_2 = 0.004, r_0 = 0.015, and r_∞ = 0; trace v, ϕ_1 = 18.7 μs, ϕ_2 = 233.0 μs, β_1 = 0.010, β_2 = 0.005, r_0 = 0.033, and r_∞ = 0.018. The concentrations of actin and cytochalasin B were 1.0 mg/mL and 1.0 μM, respectively.

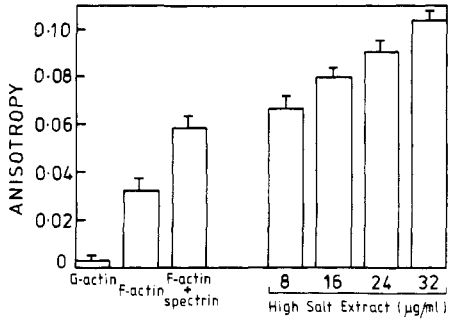

FIGURE 3: Time-invariant anisotropies of G-actin and polymerized actin in the presence and absence of spectrin dimer and a preparation (high-salt extract) containing equal amounts (micrograms per milliliter) of bands 2.1 and 4.1. The spectrin was mixed gently with a sample of polymerized actin, and this was followed by increasing amounts of the high-salt extract. The concentrations of actin and spectrin were 1.5 and 0.28 mg/mL, respectively. The temperature was 23.0 °C.

DL-arabinose. Any conversion of the spectrin dimer to tetramer under the conditions of the experiment would be expected to lead to a cross-linked network of filaments in which the rotational freedom of the phosphorescent label was further restricted.

The time-resolved anisotropy of actin samples during the formation of filaments was measured by lowering the temperature to 13 °C to decrease the rate of polymerization sufficiently to allow the collection of I_{VV} and I_{VH} decays within a short time period (approximately 3 min) during which there was little change in the degree of polymerization. This temperature was chosen on the basis of the rate of polymerization

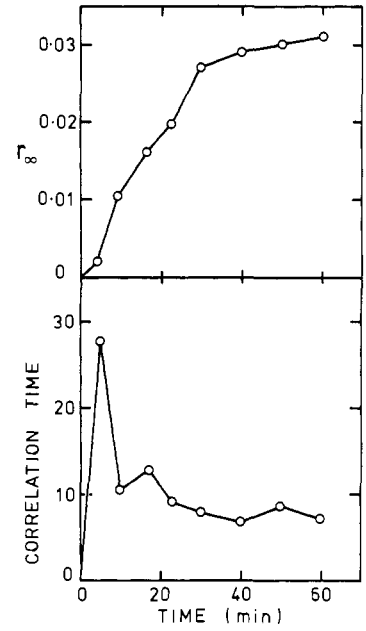

FIGURE 4: Variation of the infinite-time anisotropy (r_∞) and the rotational correlation time during the polymerization of actin at 13.0 °C. The actin concentration was 1.0 mg/mL.

measured by observing the enhancement of pyrenyl fluorescence of a separate sample of suitably labeled actin. A typical decay taken 5 min after the initiation of polymerization is shown in Figure 2 (trace iii), and values of fitted parameters (ϕ and r_∞) obtained during the course of the polymerization are summarized in Figure 4. All anisotropy decays could be fitted to a single exponential function. The correlation time reached a peak of 28 μs within 5 min of initiating polymerization and then declined sharply to values of less than 10 μs. The infinite-time anisotropy increased to 0.03 and showed evidence of the typical lag phase during the early stages of actin polymerization attributable to the formation of nucleating oligomers. The amplitude of the decay remained relatively constant (0.012 ± 0.002 SD) within the first 60 min. At longer times, the amplitude decreased, and eventually no decay was evident (Figure 2, trace i). The zero-time anisotropy therefore showed a trend similar to that seen for r_∞ within the first 60 min. As has been found elsewhere for erythrosin-labeled proteins (Zidovetzki et al., 1986), three exponentials were required to fit the total intensity decays. The time constants involved did not change appreciably during the course of the polymerization. Representative of the data is the decay 10 min after initiation of polymerization: the lifetime components were 16.9, 97, and 547 μs with fractional amplitudes of 0.30, 0.29, and 0.41, respectively.

Although the main feature of Figure 4, that is, the maximum in the correlation time occurring within 5–10 min of initiation of polymerization, was reproducible between actin preparations, considerable variation was found in the absolute values of the correlation times. Similar variations between samples were found in time-resolved anisotropy studies of fluorescently labeled actin (Tawada et al., 1978; Ikkai et al., 1979). We believe that these variations are related to the age of the actin sample and to the presence of globular aggregates of denatured actin which are known to occur when the ionic strength is increased (Rees & Young, 1967).

Analysis of Results. Significant features of Figure 4 are the maximum in the correlation time and the increasing value of r_∞ during the course of polymerization. These results, taken together with those in Figure 2 (traces i–iii), imply (a) that the short filaments formed early in the polymerization process

Table I: Phosphorescence Anisotropy Decay Parameters for a Three-Component System Used for the Simulation Shown in Figure 5[a]

component	ϕ_j (μS)	β_j	r_∞	curves x_j for (Figure 5) 1	2	3	4
1	20	0.055	0.025	0.33	0.33	0.20	
2	250	0.065	0.035	0.33	0.10		
3	∞	0.050	0.050	0.33	0.56	0.80	1.00
			$\bar{\phi}$ 135		74	20	

[a] Decays were computed according to the equation $r(t) = \sum x_j[\beta_j \exp(-t/\phi_j) + r_\infty]$ where x_j is the mole fraction of the jth component.

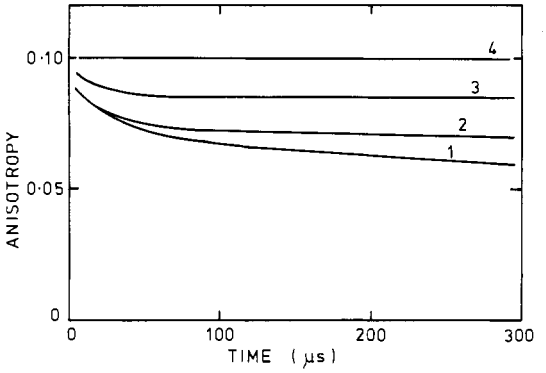

FIGURE 5: Anisotropy decays for a three-component system calculated for the decay parameters listed in Table I. The simulation refers to a situation in which component 1 rotates rapidly (ϕ_1 = 20 μs) and component 2 more slowly (ϕ_2 = 250 μs), while component 3 is rotationally immobile. In the progression from curve 1 to curve 4, components 1 and 2 are removed to form component 3 according to the fractional compositions listed in Table I.

are free to diffuse rotationally on the phosphorescence time scale, (b) that long filaments are rotationally immobile and therefore contribute a constant anisotropy to the decay profile, and (c) that the decrease in the correlation time from a maximum value is due to the presence of short filaments whose contributions to the decay profile become more obvious as longer filaments are removed into an immobile state. Failure to see an anisotropy decay in samples in which polymerization has been allowed to proceed to an equilibrium position (Figure 2, trace i) would indicate that under these conditions the majority of filaments, be they short or long, are rotationally immobile.

A data simulation exercise was carried out to clarify these possibilities. A three-component system was generated; the first two components had rotational correlation times of 20 and 250 μs while the third population was completely immobile. Appropriate values were chosen for the decay amplitudes and the intrinsic infinite-time anisotropies of each component. It was assumed that the phosphorescence lifetimes were similar for all components. The decay parameters are listed in Table I, and the simulated decays are shown in Figure 5. When the three components are present in equal proportion, the anisotropy decay reflected the mobility of the two mobile components (Figure 5, curve 1). When the proportion of the second component was decreased with a corresponding increase in the proportion of the third or immobile component, there was a rise in the infinite-time anisotropy, and the first component started to dominate the decay (Figure 5, curve 2). When all of component 2 (and some of component 1) was converted to component 3, only component 1 contributed to the decay kinetics (Figure 5, curve 3). Finally, when components 1 and 2 were converted completely to component 3, then there was no rotational relaxation, and the anisotropy remained constant with time (Figure 5, curve 4). During this process, the weight-average correlation time ($\bar{\phi}$), which is defined as $\sum_i c_i\phi_i/\sum_i c_i$, where c_i is the weight concentration of the ith species, decreases from 135 to 20 μs (Table I).

This simulation, although based on an exaggerated and simplified model, assists our understanding of the correlation time profile shown in Figure 4 in terms of changes in the relative populations of the rotating and immobile species present. In particular, it explains the rise in the apparent correlation time to a maximum and the subsequent decline. However, there are two important qualifications. The first is that the simulation does not allow for an increase in the proportion of short filaments, merely the removal of a subpopulation of filaments into an immobile state. The second is that the simulation treats a three-component mixture whereas F-actin itself is polydisperse with respect to filament length. Although the experimental decays of anisotropy were fitted to a single exponential function, this situation has no physical significance and appears to be the consequence of the spectrum of filament lengths and of the corresponding distribution of correlation times. Another source of such a dispersion in the anisotropy decay resides in the multiexponential nature of the total intensity decay. Under these conditions, the observed value of $r(t)$ is a time-dependent average of anisotropies, each weighted by a corresponding intensity decay. The fact that the intensity decay parameters remained relatively constant during the polymerization process lends further weight to the view that the changes in the kinetics of the anisotropy decay are due to changes in the distribution of filament length and not to changes in the intrinsic photophysical properties of the probe.

Kawamura and Maruyama (1970) have used the electron microscope to measure the length distribution of filaments at various stages during the polymerization process. Their experiments show that although the number-average and weight-average filament lengths increase during polymerization, the proportion of short filaments (<1 μm) increases significantly, as predicted by the theoretical treatment of Oosawa and Asakura (1975), although fragmentation of longer filaments might also be a contributing factor. For example, the percentage of filaments less than 0.5 μm in length increased from 20% at 3 min to 36% at 190 min. Using their results, we calculated the rotational correlation time for each length category assuming that the filament rotates as a rigid rod. The diffusion of a rigid rod about its long axis ($D_\parallel$) is given by

$$D_\parallel = k_B T/4\pi\eta r^2 l \quad (6)$$

$$\phi = 1/D_\parallel \quad (7)$$

where k_B is Boltzmann's constant, r the radius of the rod, l its length, and η the solvent viscosity (Broersma, 1960). The weight-average correlation time ($\bar{\phi}$) can then be calculated as discussed above.

The results are shown in Figure 6 and are in accord with our experimental findings, particularly with respect to the maximum which occurs in the correlation time profile. The experimentally determined correlation times are shorter than those derived from electron microscopy, but this may reflect different conditions of polymerization or sample treatment. If it is assumed that filaments above a given length are im-

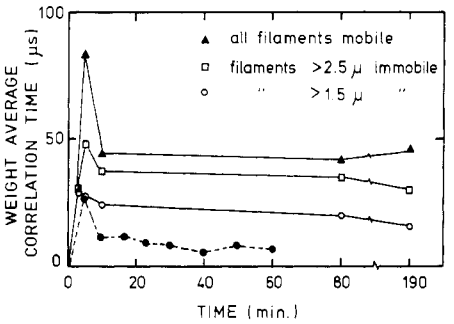

FIGURE 6: Weight-average correlation time of actin during the course of polymerization calculated from the data of Karamura and Maruyama (1970) for situations in which filaments of different length become immobile. See text for details. The data of the present study are superimposed for comparison (dashed line).

mobile due to their contact and mutual entanglement, then the height of the peak maximum is reduced, and eventually the peak disappears when filaments greater than 1.5 μm long are considered to be immobile. The true situation is probably more complex since it is possible that the length at which filaments become rotationally immobile changes during the course of polymerization. For example, the absence of an anisotropy decay in F-actin at equilibrium does not necessarily mean that short filaments (<0.5 μm) are not present but rather that all filaments, short and long, are immobile in the F-actin gel.

The extraction of a weight-average correlation time from the filament length distributions determined by electron microscopy is an approximate treatment designed to show the trends in the correlation time during the polymerization reaction. However, the uniaxial rotation of a rigid rod will illicit an anisotropy decay with two time constants, one of which is 4 times the other (Rigler & Ehrenberg, 1973). Only the shorter correlation time is used for the comparison depicted in Figure 6.

Effect of Protein Concentration and Temperature. As discussed above, solutions of F-actin at equilibrium show a time-independent anisotropy (Figure 2, trace i). This anisotropy was dependent on the actin concentration and varied monotonically from 0.06 at 0.1 mg/mL to 0.10 at 2.0 mg/mL, indicating a progressive restriction of the range of angular motions of the probe. This change was not associated with any decay on the phosphorescence time scale and must therefore arise from restriction of the submicrosecond torsional motion in the actin filament, presumably due to interfilament interactions. Measurements on the fluorescence time scale support this interpretation. Tadawa et al. (1978) found that a long correlation time associated with actin labeled with a naphthyl fluorophore increased with increasing actin concentration. This is to be expected for a system where rotationally mobile G-actin makes less and less of a contribution to the overall decay. However, these authors also suggested that the increased correlation time was due to the interaction of filaments causing a restriction of internal deformation motions within the fiber, a conclusion which was confirmed later in a more extensive study (Ikkai et al., 1979). This interpretation is in agreement with the concentration-dependent increase in anisotropy on the phosphorescence time scale reported in the present study.

Measurements of translational diffusion using the photobleaching recovery technique have shown that at moderate actin concentrations (>0.25 mg/mL) the lateral immobilization of filaments is complete but that at low concentrations of actin (0.05 ml/mL) immobilization of filaments is only partial, reflecting a decreased probability of forming filament

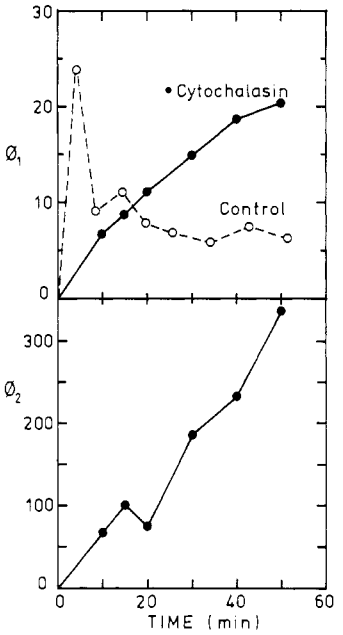

FIGURE 7: Changes in the correlation times (ϕ_1 and ϕ_2) of actin (1 mg/mL) polymerized in the presence of cytochalasin B (1 μM). The data for the single exponential fits for the control (no cytochalasin) are included in the upper panel for comparison.

crossovers and networks (Tait & Frieden, 1982a). The anisotropy results discussed above suggest that at low concentrations, the filaments are also more rotationally mobile such that submicrosecond torsional motion of the filaments leads to lower anisotropy values on the phosphorescence time scale.

Further information on interfilament interactions was sought by examining the temperature dependence of the anisotropy at low and high actin concentrations. We found that whereas the anisotropy at the higher concentration (1.0 mg/mL) was largely independent of temperature in the range 10–40 °C, the anisotropy at the lower concentration (0.1 mg/mL) showed a linear decline with increasing temperature (r = 0.07 at 10 °C to r = 0.04 at 40 °C). As was noted previously, the phosphorescence anisotropies were independent of time, even at the highest temperature. The results suggest that at the lower actin concentration, interactions between filaments, which may restrict the submicrosecond depolarization of the emission, are weaker at the higher temperature, so leading to lower anisotropies. This effect is not seen at the higher actin concentration where filament entanglement would seem to be substantial enough to restrict the torsional motion of filaments even at the higher temperatures. The critical actin concentration tends to decrease with increasing temperature (Gordon et al., 1976), and thus the contribution of G-actin to the anisotropy cannot explain the temperature dependence noted at the lower protein concentration.

Effect of Cytochalasin B. Significant changes occurred to the time-resolved anisotropy of erythrosin-labeled actin when it was polymerized in the presence of 1.0 μM cytochalasin B. The anisotropy decay measured 30 min after the initiation of polymerization is shown in Figure 2 (trace iv). It is characterized by a double exponential decay with correlation times of 10.8 and 104 μs. The decay data collected during the course of the polymerization are summarized in Figure 7. A steady increase occurred in the shorter lifetime component from 7–10 μs at 10 min to 20 μs at 50 min after the initiation of polymerization. However, the most substantial change occurred in the longer correlation time which increased 5-fold between 10 and 50 min. The value of r_∞ increased to approximately 0.02 during polymerization. The two amplitudes showed a slight

decrease over 60 min and were very small by 120 min (<0.01 each). Under these circumstances, the decay time is difficult to measure due to the low signal to noise ratio coupled with a long correlation time.

Electron microscopy shows that cytochalasin B slows or blocks elongation of F-actin at the barbed end of the filament (McLean-Fletcher & Pollard, 1980; Pollard & Mooseker, 1981). Consequently, filaments are shorter, and the steady-state intrinsic viscosity is lower (Hartwig & Stossel, 1979). In terms of rotational motion, the main effect of treatment with cytochalasin B is to remove the maximum in the ϕ versus time curve (Figure 4). We conclude that cytochalasin treatment abolishes the buildup of short rotationally mobile filaments discussed above and leads to the accumulation of filaments of intermediate size which are also rotationally mobile but have correlation times longer (100–400 μs) than those of the population of short filaments. The final value of r_∞ was lower than the control (0.016 compared to 0.030). This would be expected if the submicrosecond internal motion in the shorter capped filaments was less hindered due to fewer contacts between filaments and less intermeshing of filaments.

Summary and Concluding Comments. Solutions of F-actin appear to be rotationally immobile on the millisecond time scale due to entanglement and contact of filaments. Rapid bending and torsional motion on the submicrosecond time scale contribute to the initial depolarization of the phosphorescence anisotropy signal and to relatively low values of the zero-time anisotropy. Formation of a spectrin dimer–F-actin complex appears to limit the submicrosecond motions, leading to additional increases in the anisotropy. Addition of a preparation containing erythrocyte membrane components 2.1 and 4.1 leads to further increases in the anisotropy. An important finding is that the correlation time measured during actin polymerization is sensitive to the length distribution of filaments.

The rotational motion of F-actin has also been measured by using saturation-transfer ESR. Thomas et al. (1979) determined a correlation time of 100 μs for such motion although they point out that the estimate was based on a comparison of spectra with theoretical and experimental spectra corresponding to isotropic rotational diffusion. In both the saturation-transfer ESR and phosphorescence anisotropy methods, the ability to detect molecular motion depends on the orientation of the probe relative to the rotational axis of the molecule. The angle between the triplet emission moment and the axis of rotation of the actin filament is not known, and a more extensive analysis of the system will have to await the extraction of such information from experiments with oriented systems.

Our conclusions with respect to F-actin differ from those reported by Yoshimura et al. (1984). These authors measured the absorption dichroism and phosphorescence anisotropy of eosin-labeled F-actin and reported a single relaxation time of about 450 μs which they interpreted as indicating torsional motion within the filament. We have been unable to detect such motion. The origin of these differing results is not clear. However, we note that their samples were deoxygenated by purging with argon and were stirred within the cuvette for 10 min before each measurement. Such treatment disrupts the F-actin gel. In our hands, this treatment also leads to the formation of denatured particles in the cuvette and to a variety of artifactual anisotropy decays, including, at times, the observation of rising anisotropies. Enzymic deoxygenation with glucose oxidase, as used in the experiments reported in the present paper, has the advantage that the actin solution is not disturbed by mixing either during or at the completion of the polymerization process, thereby avoiding the formation of denatured aggregates. We also note the desirability of using actin solutions which are spiked with the minimum amount of labeled monomers since Yoshimura et al. (1984) show that the labeled protein polymerizes less efficiently than the unlabeled material as judged by viscosity measurements [see also Tait and Frieden (1982b)].

ACKNOWLEDGMENTS

We thank Drs. A. Husain, R. Learmonth, and L. Tilley for helpful discussion of this work. We are most grateful to Dr. T. M. Jovin for the generous use of his triplet spectrometer at Gottingen to carry out additional anisotropy measurements of F-actin.

REFERENCES

Austin, R. H., Chan, S. S., & Jovin, T. M. (1979) *Proc. Natl. Acad. Sci. U.S.A. 76*, 5650–5654.

Bevington, P. R. (1969) *Data Reduction and Error Analysis for the Physical Sciences*, McGraw-Hill, New York.

Broersma, S. (1960) *J. Chem. Phys. 32*, 1626–1631.

Cherry, R. J., & Schneider, G. (1976) *Biochemistry 15*, 3657–3661.

Cohen, C. M., & Foley, S. F. (1980) *J. Cell Biol. 86*, 694–698.

De Boeck, H., Macgregor, R. B., Clegg, R. M., Sharon, N., & Lootiens, F. G. (1985) *Eur. J. Biochem. 149*, 141–145.

Garland, P. B., & Moore, C. H. (1979) *Biochem. J. 183*, 561–572.

Gordon, D. J., Yang, Y.-Z., & Korn, E. D. (1976) *J. Biol. Chem. 251*, 7474–7479.

Hartwig, H., & Stossel, T. P. (1979) *J. Mol. Biol. 134*, 539–553.

Ikkai, T., Wahl, P., & Auchet, J. C. (1979) *Eur. J. Biochem. 93*, 397–408.

Jovin, T. M., Bartholdi, M., & Vaz, W. L. C. (1981) *Ann. N.Y. Acad. Sci. 366*, 176–196.

Kawamura, M., & Maruyama, K. (1970) *J. Biochem. (Tokyo) 67*, 437–457.

Kawasaki, Y., Mihashi, K., Tanaka, H., & Ohnuma, H. (1976) *Biochim. Biophys. Acta 446*, 166–178.

Kuntz, I. D. (1971) *J. Am. Chem. Soc. 93*, 516–518.

Lanni, F., & Ware, B. R. (1984) *Biophys. J. 46*, 97–110.

Lanni, F., Taylor, D. L., & Ware, B. R. (1981) *Biophys. J. 35*, 351–364.

MacLean-Fletcher, S., & Pollard, T. D. (1980) *Cell (Cambridge, Mass.) 20*, 329–341.

Malachowski, G., & Ashcroft, R. (1986) *Proceedings of the Australian Society of Biophysics*, 10th Annual Meeting, p 19, Canberra, Australia.

Mihashi, K., & Wahl, P. (1975) *FEBS Lett. 52*, 8–12.

Moore, C., Boxer, D., & Garland, P. (1979) *FEBS Lett. 108*, 161–166.

Mozo-Villarias, A., & Ware, B. R. (1985) *Biochemistry 24*, 1544–1548.

Niederman, R., Amrein, P. C., & Hartwig, J. (1983) *J. Cell Biol. 96*, 1400–1413.

Oosawa, F. (1980) *Biophys. Chem. 11*, 443–446.

Oosawa, F., & Asakura, S. (1975) *Thermodynamics of the Polymerization of Proteins*, Academic, New York.

Pollard, T. D., & Mooseker, M. S. (1981) *J. Cell Biol. 88*, 654–659.

Rees, M. K., & Young, M. (1967) *J. Biol. Chem. 242*, 4449–4458.

Restall, C. J., Dale, R. E., Murray, E. K., Gilbert, C. W., & Chapman, D. (1984) *Biochemistry 23*, 6765–6776.

Rigler, R., & Ehrenberg, H. (1973) *Q. Rev. Biophys. 6*, 139–199.
Sawyer, W. H., Hill, J. S., Howlett, G. J., & Wiley, J. S. (1983) *Biochem. J. 211*, 349–356.
Spudich, J. A., & Watt, S. (1971) *J. Biol. Chem. 246*, 4866–4871.
Tait, J. F., & Frieden, C. (1982a) *Biochemistry 21*, 3666–3674.
Tait, J. F., & Frieden, C. (1982b) *Arch. Biochem. Biophys. 216*, 133–141.
Tawada, K., Wahl, P., & Auchet, J. C. (1978) *Eur. J. Biochem. 88*, 411–419.
Thomas, D. D., Seidel, J. C., & Gergely, J. (1979) *J. Mol. Biol. 132*, 257–273.
Timmermans, J. (1960) in *Physico-Chemical Constants of Binary Systems in Concentrated Solutions*, Vol. 4, pp 252–267, Interscience, New York.
Wahl, P., Mihashi, K., & Auchet, J. C. (1975) *FEBS Lett. 60*, 164–167.
Yguerabide, J. (1972) *Methods Enzymol. 26*, 498–578.
Yoshimura, H., Nishio, T., Mihashi, K., Kinosita, K., & Ikegami, A. (1984) *J. Mol. Biol. 179*, 453–467.
Zidovetski, R., Bartholdi, M., Arndt-Jovin, D., & Jovin, T. M. (1986) *Biochemistry 25*, 4397–4401.

Time-Resolved Fluorescence Investigation of Membrane Cholesterol Heterogeneity and Exchange†

Gyorgy Nemecz‡ and Friedhelm Schroeder*,‡,§

Division of Pharmacology and Medicinal Chemistry, College of Pharmacy, Department of Pharmacology and Cell Biophysics, College of Medicine, University of Cincinnati Medical Center, Cincinnati, Ohio 45267-0004

Received March 22, 1988; Revised Manuscript Received June 21, 1988

ABSTRACT: The fluorescent sterol $\Delta^{5,7,9(11),22}$-ergostatetraen-3β-ol (dehydroergosterol) was investigated as a cholesterol analogue to examine sterol domains in and spontaneous exchange of sterol between 1-palmitoyl-2-oleoylphosphatidylcholine (POPC) small unilamellar vesicles (SUV). Fluorescence lifetime, acrylamide quenching analyses, and intermembrane exchange kinetics were consistent with the presence of at least two sterol domains in POPC. Fluorescence lifetime was determined by phase and modulation fluorescence spectroscopy and analyzed by nonlinear least-squares as well as continuous distributional analyses. Both methods demonstrated that pure dehydroergosterol in POPC SUV had two lifetime components (C) and fractional intensities (F) near C_1 = 0.851 ns (F_1 0.96) and C_2 = 2.668 ns (F_2 0.04). In contrast to component C_1, the center of lifetime distribution, fractional intensity, and peak width of dehydroergosterol lifetime component C_2 was dependent on the polarity of the medium and vesicle curvature. The sterol domain corresponding to dehydroergosterol component C_2 was preferentially quenched by acrylamide. Acrylamide quenching of dehydroergosterol fluorescence demonstrated that the two lifetime components of dehydroergosterol were not due to transbilayer sterol domains with different lifetimes. In a spontaneous exchange assay not requiring separation of donor and acceptor SUV, the lifetime component C_2, but not C_1, shifted to a shorter lifetime with altered distributional width. The kinetics of these lifetime and distributional width changes best fitted a two-exponential function, with a fast exchange rate constant k_1 = 0.0325 min^{-1}, $t_{1/2}$ = 21.3 min, and a slow rate constant k_2 = 0.00275 min^{-1}, $t_{1/2}$ = 261 min. The fast exchanging pool correlates with the longer lifetime component C_2. These kinetics were confirmed both by dehydroergosterol exchange measured with fluorescence intensity and by [^{3}H]cholesterol exchange. In summary, lifetime, distributional width, acrylamide quenching, and classical exchange assay data are consistent with the presence of at least two pools of sterol in POPC SUV.

Recently the fluorescent sterol dehydroergosterol[1] gained popularity as a probe molecule for monitoring the structural and rotational dynamic properties of cholesterol in model membranes (Rogers et al., 1979; Hale & Schroeder, 1982; Yeagle et al., 1982; Schroeder, 1984; Fischer et al., 1985a; Smutzer et al., 1986; Chong & Thompson, 1986; Schroeder et al., 1987), biological membranes (Schroeder, 1981; Hale & Schroeder, 1982; Muczynski & Stahl, 1983; Kier et al., 1986), and lipoproteins (Smith & Green, 1974; Schroeder et al., 1979a,b; Yeagle et al., 1982). In addition, dehydroergosterol was used to examine sterol–protein interactions with cytosolic sterol carrier protein (Fischer et al., 1985b), membrane glycophorin (Yeagle et al., 1982), and plasma lipoprotein apoproteins (Smith & Green, 1974b).

Despite these observations, only one report utilized dehydroergosterol to examine the presence of sterol domains in membranes (Schroeder et al., 1987). Neither has dehydroergosterol heretofore been reported as a probe molecule for

† This work was supported in part by grants from the USPHS (GM 31651 and AA 02054).

* To whom correspondence should be addressed at the College of Pharmacy.
‡ Division of Pharmacology and Medicinal Chemistry, College of Pharmacy.
§ Department of Pharmacology and Cell Biophysics, College of Medicine.

[1] Abbreviations: POPC, 1-palmitoyl-2-oleoylphosphatidylcholine; SUV, small unilamellar vesicles; dehydroergosterol, $\Delta^{5,7,9(11),22}$-ergostateraen-3β-ol.

0006-2960/88/0427-7740$01.50/0